Article

Organic/Inorganic Hybrid Materials Formed From TiO$_2$ Nanoparticles and Polyaniline

Danielle C. Schnitzler and Aldo J. G. Zarbin*

Departamento de Química, Universidade Federal do Paraná, CP 19081, 81531-990 Curitiba - PR, Brazil

Este artigo descreve a síntese e caracterização de diferentes híbridos orgânico/inorgânicos formados entre a polianilina e o óxido de titânio. O método de preparação é baseado no processo sol-gel, partindo do isopropóxido de titânio como precursor. Duas rotas sintéticas visando a obtenção dos híbridos foram utilizadas, baseadas na mistura da anilina no meio reacional antes ou após a formação do óxido. Diferentes quantidades de anilina foram utilizadas visando compreender este efeito nas características do material final formado. As amostras foram caracterizadas por análise térmica, difratometria de raios-X, espectroscopias Raman, UV-Vis em modo reflectância difusa e IV-TF, além de voltametria cíclica. Os resultados indicaram que os diferentes procedimentos experimentais foram bem sucedidos na obtenção de híbridos formados por nanopartículas de TiO$_2$ (estrutura anatase) e polianilina em sua forma condutora, sal esmeraldina. Não foram detectadas grandes diferenças entre as amostras obtidas através das duas rotas sintéticas utilizadas, exceto pela quantidade de polímero formada nos materiais.

This paper describes the synthesis and characterization of organic/inorganic hybrid materials formed from TiO$_2$ nanoparticles and polyaniline (PANI). The preparation method is based on a sol-gel technique using titanium tetra-isopropoxide as oxide precursor, and two synthetic routes to the hybrids formation were employed, based on the addition of aniline after or before the sol formation. Different amounts of aniline were used to verify this effect on the characteristics of the formed materials. Samples were characterized by electronic spectroscopy, Raman spectroscopy, Fourier transformed infrared spectroscopy, thermal analysis, X-ray diffractometry and cyclic voltammetry. Results show that the different experimental routes are successful to produce hybrids formed by oxides nanoparticles and polyaniline in its conducting form, the emeraldine salt. There are no strong differences between the samples obtained by the two synthetic routes employed, except by the amount of polymer in the final material.

Keywords: sol-gel method, polyaniline, nanocomposites

Introduction

Interest in the development of new inorganic/organic (nano)composites has grown in recent years due to a wide range of potential use of these materials.[1-10] These hybrids constitute a class of advanced composite materials with unusual properties, which can be used in many fields such as optics, ionics, electronics, mechanics *etc*.

One important class of hybrid materials is that in which the organic fraction is composed by conducting polymers, such as polyaniline (PANI) or polypyrrole.[11-19] The unique properties of hybrid materials become more pronounced when at least one of the fractions occurs in nanometric scale. Nanocomposites in which the polymer fraction occurs in nanometric scale can be obtained by the encapsulation of conducting polymers within void spaces of inorganic host matrices such as pores, cavities, tunnels, micelles and interlayer domains.[12,13,18,19] We have recently prepared polypyrrole and polyaniline nanocomposites with several inorganic matrices like porous glasses,[20-22] layered materials[23,24] and three-dimensional framework materials.[25]

Another interesting type of nanocomposites is that in which the inorganic material represents the nanometric phase. By this way, a great number of nanocomposites between conducting polymers and nanoparticles of different oxides as TiO$_2$, Fe$_2$O$_3$ and SnO$_2$ have been described.[26-33] Several reports involving the synthesis and characterization of different polypyrrole or polyaniline/TiO$_2$ hybrids have been described aiming to obtain materials that find applications in electrochromic devices, nonlinear optical systems, photoelectrochemical devices *etc*.[29,34-38] For

* e-mail: aldo@quimica.ufpr.br

example, the combination of the n-type semiconductor property of nanoparticulated TiO$_2$ with the p-type of polyaniline has been considered as responsible for an improvement in the polyaniline photocurrent values due to the occurrence of exciton dissociation at their interface.[30]

TiO$_2$/conducting polymer hybrids have been prepared by the electrochemical polymerization of the monomer on a film of the oxide,[36,37] or by chemical polymerization of the monomer in a dispersion which contains the oxide (nano)particles.[26,30,33,34,39] The experimental procedure is fundamental to control the properties of the resulting material. Variables like size and shape of the oxide particles, degree of the dispersion, kind of interaction and interface between the organic and the inorganic phases, among others, have direct influence on properties like conductivity, piezoresistivity, photocurrent, etc. Recently we reported the *in situ* synthesis and characterization of some hybrid materials between (Ti,Sn)O$_2$ nanoparticles and the conducting polymer polyaniline.[40] In this paper we report similar approach to hybrids between TiO$_2$ nanoparticles obtained by the sol-gel route and polyaniline. Two different synthetic approaches were used based on the addition of aniline before or after the hydrolysis of the oxide precursor. Also, the effect of the initial amount of aniline added to the system in the characteristics of former hybrid materials was studied.

Experimental

Titanium oxide was prepared based on method described by Bischoff and Anderson.[41] 10 mL of titanium tetra-isopropoxide (TTIP – Strean product), used without further purification, was diluted in 30 mL of isopropanol (Carlo Erba). This mixture was added in 50 mL of MilliQ filtered H$_2$O into which 0.5 mL of concentrated chloridric acid (Merck) was previously added. Precipitation occurred immediately. The precipitate was then peptized with the available HNO$_3$ at 60 °C for 8 h in a reflux system. After this the reaction was stirred for 8 h at room temperature, followed by evaporation of isopropanol and water at 55 °C for a week. The 55 °C drying gel was stored in a desiccator for further characterization.

Two different routes were used to produce the oxide/PANI hybrids as follows:

Group 1: aniline was added previously to hydrolysis. In a glove box a suitable amount of fresh distilled aniline (0.242 or 0.675 mL) was added to the above described solution formed from TIPP. The new mixture of aniline and TIPP in isopropanol was subsequently added to react with water in a similar way as described above for the synthesis of TiO$_2$. The formed white precipitate was also peptized at

60 °C for 8 h following by stirring at room temperature for additional 8 h. After this, in order to polymerize the aniline, 30 mL of a (NH$_4$)$_2$S$_2$O$_8$ aqueous solution containing 1.0 mol L^{-1} of HCl was added to the reactional media, and the mixture was stirred at room temperature for 3 h. The (NH$_4$)$_2$S$_2$O$_8$ solution was prepared in order to maintain the aniline/ (NH$_4$)$_2$S$_2$O$_8$ molar ratio constant, by the dissolution of 0.301 or 0.851 g of (NH$_4$)$_2$S$_2$O$_8$ (to aniline amount of 0.242 or 0.675 mL, respectively) in 30 mL of a 1.0 mol L^{-1} HCl aqueous solution. The resulting green solid was separated by centrifugation, washed five times with distilled water, dried at 40 °C for a week and stored in desiccator for further characterization. The sample obtained with the minor initial amount of aniline (0.242 mL) will be referred here as TiO$_2$/PANI-1A, and the sample obtained with the higher amount of aniline (0.675 mL) as TiO$_2$/PANI-1B.

Group 2: aniline added after the hydrolysis and peptization. After all the synthetic steps to the synthesis of TiO$_2$ described above, and before the evaporation of isopropanol and water, a suitable amount of freshly distilled aniline (0.242 or 0.675 mL) was added to the media containing the TiO$_2$ sol. After 10 min under stirring, 30 mL of the same (NH$_4$)$_2$S$_2$O$_8$ solution described in the Group 1 was added to the system. The mixture was stirred at room temperature for 3 h, and the resulting green solid was separated, washed, dried and stored as described above. The sample obtained with the minor initial amount of aniline (0.242 mL) will be referred here as TiO$_2$/PANI-2A, and the sample obtained with the higher amount of aniline (0.675 mL) as TiO$_2$/PANI-2B.

XRD patterns were obtained in a Shimadzu XRD-600 diffractometer, using Co-Kα radiation with 40 kV and 40 mA, at 0.2° scan rate (in 2θ). The room temperature measurements were performed with the samples spread on a conventional glass sample holder. Powder silicon reflections were used for 2θ calibration. The areas of the XRD peaks were evaluated by Gaussian decovolution using the Origin 5.0 program. The crystallite diameter was determined employing peak-broadening analysis utilizing Scherrer's equation.

The FT-IR spectra of the samples were obtained with a Bomem MB-100 spectrophotometer in the 4000-400 cm^{-1} range with 32 scans. The samples were prepared into KBr pellets.

The Raman spectra were obtained in a Renishaw Raman Image Spectrophotometer, coupled to an optical microscope that focuses the incident radiation down to an approximately 1 μm spot. A He-Ne laser (emitting at 632.8 nm) was used, with incidence potency of 2 mW over the 2000-100 cm^{-1} region. The Raman spectra were baseline corrected using the program Origin 5.0.

TGA/DSC measurements were carried out simultaneously in a Netzsch STA 409 equipment, in static air (with no air flow). Approximately 15 mg of each sample were analyzed between 20 and 1000 °C at 8 °C min⁻¹ using alumina crucibles.

The UV-Vis spectra were collected in reflectance mode in a Shimadzu UV-2401 spectrophotometer, in the 190-900 nm region with the samples in powder, using BaSO₄ as reference.

In order to measure the cyclic voltammetry, samples (~ 0.01 g) were suspended in 2 mL of distilled water and sonicated for 15 min. 300 μL of this suspension was carefully transferred to the surface of conducting glass electrodes (ITO, CG 611N, Sheet Resistance 15-30 ohm, nominal transmittance higher than 78%, coating thickness 600-1000 Å). After water evaporation (at room temperature) a uniform and transparent film was formed inside the ITO surface, which was used as work electrode. Measurements were performed using a EG&G Princeton potentiostat, model 273A, interfaced to a PC computer. A one compartment cell with a Pt wire as counter electrode, a Ag/AgCl reference electrode and a 1 mol L⁻¹ HCl/NaCl aqueous solution as electrolyte were used. The scan speed was 50 mV s⁻¹ and the potential range from -200 to 1000 mV.

Results and Discussion

For the synthesis of the four hybrids, we introduced modifications in the synthetic procedure for the TiO₂ in two different approaches. In a first one, we mixed the monomer aniline with the molecular precursors to the oxide, and the hydrolysis was realized in this mixture. In this case, the oxide formation occurs in an environment that already contains the monomer. Second, we obtained the TiO₂ solution and then added the aniline to it. In both cases the polymerization was realized using an acidic solution of ammonium persulfate. All the polymerizations were conduced in the same way, in order to compare the characteristics of the different samples obtained. Also, for each synthetic approach, two amounts of aniline were added, aiming to obtain hybrids with different ratios between the inorganic and organic fraction, and to investigate the effect of the initial aniline amount in the final product.

The thermal behavior of the hybrid samples was investigated by thermogravimetry (TG) and differential scanning calorimetry (DSC), and the results are shown in Figure 1. The 21.5% weight loss observed until 400 °C in the TG curve of pure TiO₂ (Figure 1a) is attributed to the elimination of adsorbed water and alcohol and to the dehydroxilation process of surface-attached H₂O and OH

groups, as reported before[42]. The hybrids TG curves also show weight losses between 30-300 °C attributed to the loss of water (from both the oxide and polymer surface) and acid dopant,[43-45] besides a well-differentiated behavior marked by a strong weight loss in the 330-540 °C, attributed to degradation of the skeletal polyaniline chain structure.[43-45] This weight loss is correlated with two strong exothermic peaks in the DSC of the hybrid samples, at 388 and 504 °C, as can be seen in the inset of Figure 1. The DSC curve (which is representative for all the other hybrid samples) also show an endothermic peak centered at 88 °C (due the water loss of system) and an exothermic peak at 687 °C attributed to a anatase-rutile phase transition in the titanium oxide.[42]
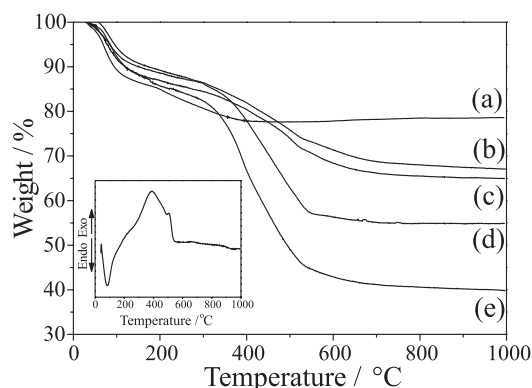

Figure 1. Termogravimetric curves, obtained in air atmosphere at 8 °C min⁻¹: (a) TiO₂; (b) TiO₂/PANI-2A; (c) TiO₂/PANI-1A; (d) TiO₂/PANI-2B; (e) TiO₂/PANI-1B. The inset shows the DSC curve for TiSn/PANI-1A sample.

Based on the TG data we can estipulate the amount of polyaniline in each hybrid sample, which corresponds to the following (in weight percent): 18.0; 39.5; 17.0 and 30.0 for the samples TiO₂/PANI-1A, TiO₂/PANI-1B, TiO₂/PANI-2A and TiO₂/PANI-2B respectively.

The green color of all the four samples obtained was the first evidence of the polyaniline formation in its conducting form, emeraldine salt (ES). The ES occurrence was confirmed by infrared (FT-IR), Raman and reflectance UV-Vis spectroscopy. The FT-IR spectra of the hybrid samples (Figure 2) present all the characteristics bands of ES, at 1611, 1573, 1484, 1307, 1241, 1139, 1051, 985 and 808 cm⁻¹.

Figure 3 shows the Resonance Raman spectra of hybrids and of the pure oxide. These spectra were collected with the 632.8 nm laser, which frequency is coincident with the visible absorption band assigned to the radical cation segment, as will be discussed after. By this way, as expected, the quinoid and semiquinoid Raman bands are very salient in the spectra. As we can see on Figure 3, all
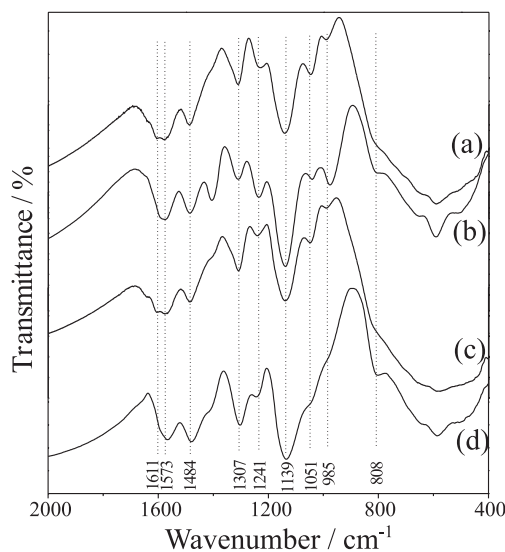
Figure 2. Infrared spectra: (a) TiO$_2$/PANI-1A; (b) TiO$_2$/PANI-1B; (c) TiO$_2$/PANI-2A; (d) TiO$_2$/PANI-2B.

the hybrid spectra are very similar and are in agreement with the previously described spectra of pure emeraldine salt,[46-50] with the following main bands: ~1595 cm^{-1} (ν C=C of the quinoid rings), ~1502 cm^{-1} (ν C=N of the quinoid di-imina units), ~1339 cm^{-1} (ν C-N radical cation), ~1256 cm^{-1} (ν C-N benzene diamine units) and ~1163 cm^{-1} (C-H bending of the quinoid rings).
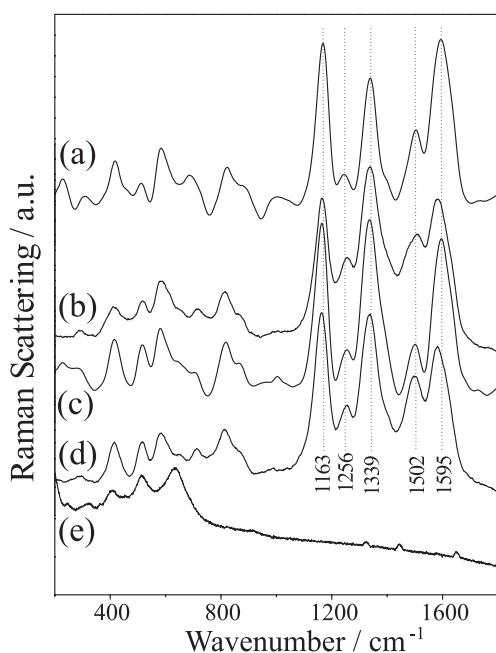

Figure 3. Resonance Raman spectra: (a) TiO$_2$/PANI-1A; (b) TiO$_2$/PANI-1B; (c) TiO$_2$/PANI-2A; (d) TiO$_2$/PANI-2B; (e) TiO$_2$.

Reflectance UV-Vis spectra of hybrid samples are shown in Figure 4. The spectrum of pure TiO$_2$ is also

showed. Clearly the hybrid samples present characteristic bands of polyaniline-emeraldine salt at ~320 nm, ~415 nm and ~700-850 nm, which are attributed to π-π^*, polaron-π^* and π-polaron transitions, respectively.[51] As can be seen on Figure 4, with increased content of polyaniline, the band attributed to the π-polaron transition is shifted from 824 and 853 nm (TiO$_2$/PANI-1A and TiO$_2$/PANI-2A) to 701 and 700 nm (TiO$_2$/PANI-1B and TiO$_2$/PANI-2B, respectively). Similar results were observed in hybrid samples obtained in a similar way, but using (Ti,Sn)O$_2$ than TiO$_2$ as the inorganic fraction.[40] These results would indicate that the polarons in the hybrids obtained with the minor amount of PANI are more delocalized than that in the other samples (as observed in secondary doped polyaniline)[51,52] and are an strong indicative that the initial amount of aniline added to the system has influence on the conformation of polyaniline chains formed in the TiO$_2$/PANI hybrids.
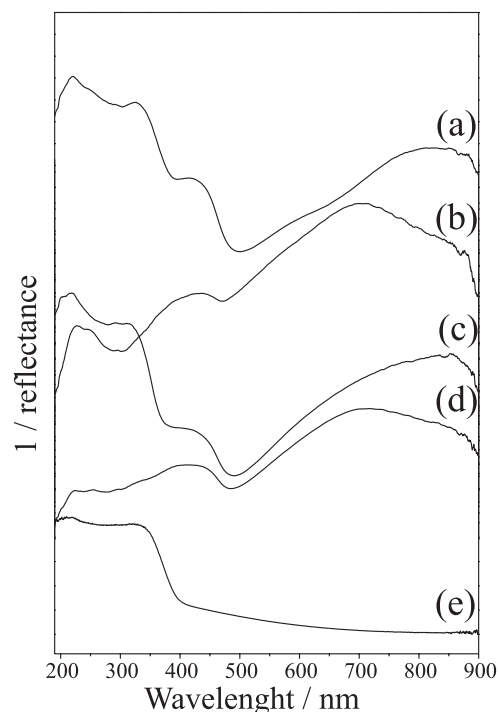

Figure 4. Reflectance UV-Vis spectra: (a) TiO$_2$/PANI-1A; (b) TiO$_2$/PANI-1B; (c) TiO$_2$/PANI-2A; (d) TiO$_2$/PANI-2B; (e) TiO$_2$.

The X-ray diffraction patterns of pure TiO$_2$ and TiO$_2$/PANI hybrids are shown in Figure 5. The oxide is formed mainly with the anatase structure (in which peaks are marked with A in the diffractogram present on Figure 5a) with traces of brookite (peaks marked with B in the Figure 5a). The XRD patterns of the hybrid samples present the same profile observed to the pure mixed oxide, indicating that the structure of oxide was not modified by the

polyaniline. Also, these results indicate that the polyaniline are amorphous in the hybrids. However the XRD profile of the sample TiO_2/PANI-1B (Figure 5c) presents, beyond the oxide peaks, four new peaks at 13.44, 19.01, 23.14 and 29.71 degrees (in 2 theta) indicating the formation of a new phase. According the TG data discussed earlier, the TiO_2/PANI-1B sample presents the higher amount of polyaniline between all the four hybrids discussed here, and despite this new phase to be not well-known, its clear that is due the improve in the PANI amount. Similar results were observed by us in hybrids formed with $(Ti,Sn)O_2$ than TiO_2 as inorganic fraction.[40] Gurunathan and Trivedi[32] and Feng *et al.*[30] also observed new peaks in the XRD pattern of hybrids formed between colloidal TiO_2 and polyaniline and attributed to a cross-linking of the polyaniline[32] or to a more ordered arrangement of the polymer in the composite samples, when compared with pure polyaniline.[30]
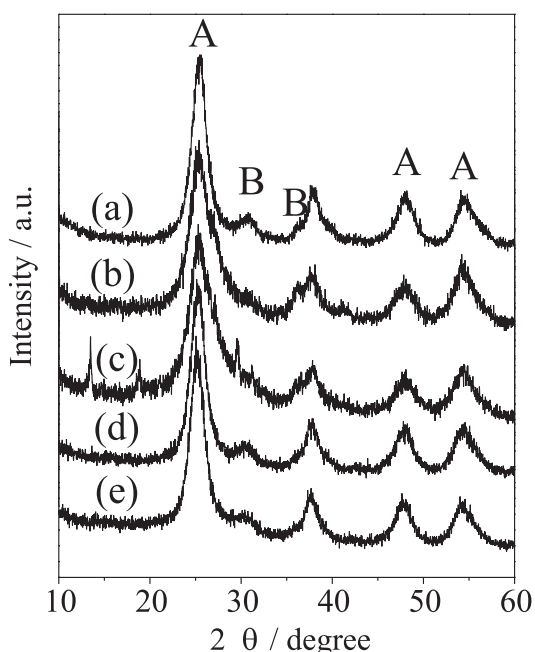

Figure 5. XRD pattern: (a) TiO_2; (b) TiO_2/PANI-1A; (c) TiO_2/PANI-1B; (d) TiO_2/PANI-2A; (e) TiO_2/PANI-2B.

The broad peaks observed in all hybrids XRD pattern indicates short crystallite diameter of the oxide, which was estimated by the Scherrer's equation as 8.7 nm. Results obtained by Scherrer's equation suggest that the TiO_2 crystallite size is not affected by the polymer presence, and is approximately the same in the pure oxide and in all the hybrids materials.

Cyclic voltammetry experiments were done and the results are shown in Figure 6. During the voltammogram acquisition, the typical polyaniline color changes were observed in all hybrid samples, showing that the materials present electrochromism. As we can see, the voltammogram of the sample TiO_2/PANI-2B shows two well-defined reversible redox processes, which are related to the typical interconversion reactions of polyaniline upon varying the potential, indicating that in this sample the main electrochemical characteristics of PANI were not significantly changed by the presence of oxide. The cyclic voltammogram of the other three hybrid samples present also the two redox pair characteristics of polyaniline, but with low definition. A poor definition of redox peaks of polyaniline was also observed earlier in polyaniline films modified by the incorporation of high amounts of platinum[53] or carbon[54] particles, and this behavior was interpreted as a strong interaction between the polymeric matrix and the incorporated particles. The significant differences observed between the cyclic voltammograms of our samples could be due the different kind of PANI/TiO_2 interactions in our different samples (resulting from the preparation methods and/or the PANI content). Another possibility can be related with the preparation of the films prior to the measurements. Although the procedure to the films preparation was the same for all the samples, it was not controlled their thickness and morphology. Also, we observed that some samples have a poor adhesion to the substrate and the films to come loose from the substrate during the measurements. Deeper studies will be necessary to clarify these points. Work to improve the overall quality of films obtained from these hybrid materials, as well as a judicious study on their electrochemical properties, will be done as soon as possible.

The results obtained by the different characterization techniques presented here can indicate that except by the resulting amount of polymer, the synthetic route employed to the hybrids (Group 1 or Group 2) does not present strong influence on the characteristics of the final product. The presence of aniline in the reactional media during the hydrolysis of the titanium isopropoxide apparently does not affect the characteristics of the former oxide. Our model to the hybrid formation is the following: the aniline monomer gets adsorbed on the oxide particles (which were well dispersed in the reactional media) and polymerization proceeds in the surface of the oxide particles when the persulphate solution was added. In the samples in which the initial amount of aniline was lower, we can suppose that all the added aniline was initially adsorbed on the oxide surface (once there are more surface available than aniline molecules to be adsorbed) and all aniline was polymerized around of oxide nanoparticles. This effect was observed in the $(Ti,Sn)O_2$/PANI hybrids recently reported by us.[40] In that case, the hybrids with the lower
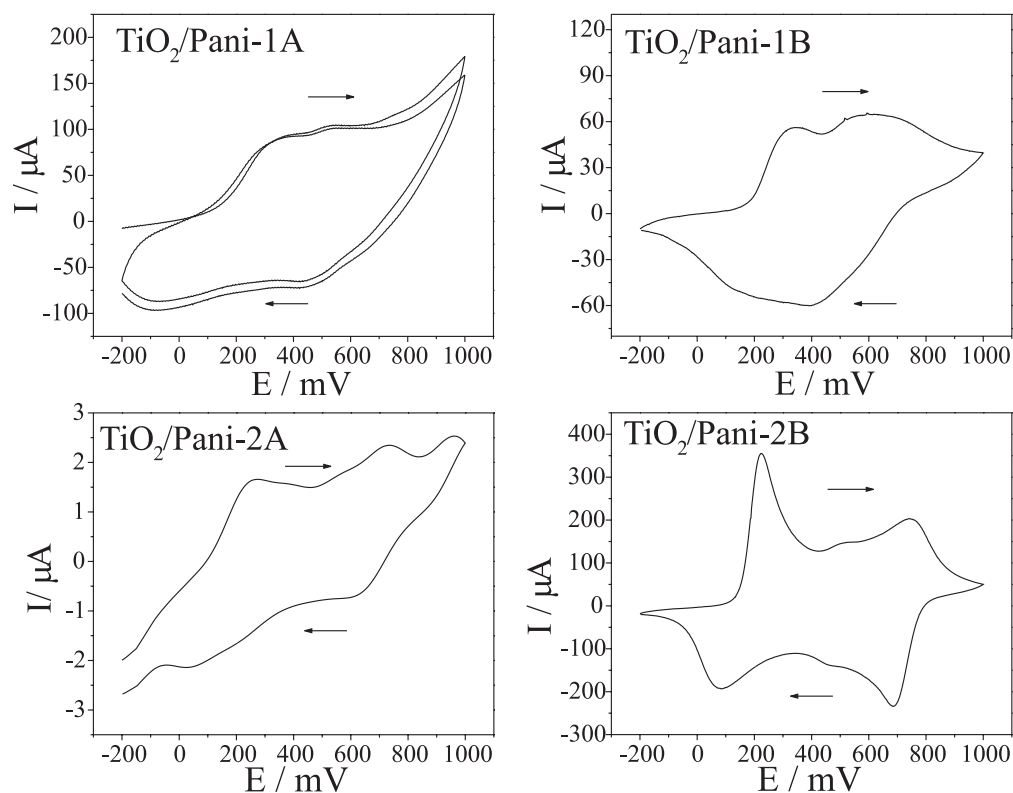
Figure 6. Cyclic voltammograms of the hybrid samples. Scan rate = 50 mV s^{-1}; electrolyte = HCl/NaCl 1.0 mol L^{-1} aqueous solution; reference electrode = Ag/AgCl.

amount of polyaniline were formed as well-defined core-shell material, in which the polymer was formed as a shell of the core oxide nanoparticles. We believe that similar effect can be occurring with the TiO_2/PANI hybrids that were formed with minor amount of polymer reported here. The growth of the polymer around the oxide surface could promote the polymer chain organization and could explain the shift of the polaronic band to higher wavenumber, as observed on Figure 4. By other way when the initial amount of aniline was higher the polymerization begins on the oxide surface and involves the excess of non-adsorbed aniline molecules, and the resulting material is formed by oxide nanoparticles incrusted in a free-polymer mass. In this configuration the polyaniline inter-chain interactions is supposed more effective, resulting in the lower wavenumber shift observed in the polaronic band.

Conclusions

Novel nanocomposites formed from TiO_2 nanoparticles and the conducting form of polyaniline were successfully obtained. The results showed here indicate that the main characteristics of the nanocomposites are not affected by the two different preparation routes presented (which was

based on the moment of aniline addition in the reactional media), but are strongly affected by the amount of monomer added prior to polymerization. This observation indicates that regardless of the aniline being present during the oxide formation or being added after it, its adsorption on the oxide surface before the polymerization apparently is the dominant step of the process. The synthetic routes described here added to the good facility to film preparation starting from the molecular precursors in the sol-gel process could open a great possibility to these materials in several devices.

Acknowledgments

References

1. Judeinstein, P.; Sanchez, C.; *J. Mater. Chem.* **1996**, *6*, 511.
2. Asefa, T.; Yoshina-Ishii, C.; MacLachlan, M.J.; Ozin, G.A.; *J. Mater. Chem.* **2000**, *10*, 1751.

3. Gomez-Romero, P.; Chojak, M.; Cuentas-Gallegos, K.; Asensio, J.A.; Kulesza, P.J.; Casan-Pastor, N.; Lira-Cantu, M.; *Elecrochem. Commun*. **2003**, *5*, 149.

4. Boury, B.; Corriu, R.J.P.; *Adv. Mater*. **2000**, *12*, 989.

5. Kimizuka, N.; Kunitake, T.; *Adv. Mater*. **1996**, *8*, 89.

6. Giannelis, E.P.; *Adv. Mater*. **1996**, *8*, 29.

7. Kryszewski, M.; *Synth. Met*. **2000**, *109*, 47.

8. Backov, R.; Bonnet, B.; Jones, D.J.; Rozière, J.; *Chem. Mater*. **1997**, *9*, 1812.

9. Choudhury, K.R.; Winiarz, J.G.; Samoc, M.; Prasad, P.N.; *Appl. Phys. Lett*. **2003**, *82*, 406.

10. Valkenberg, M.H.; Holderich, W.F.; *Catal. Rev-Sci. Eng*. **2002**, *44*, 321.

11. Kerr, T.A.; Wu, H.; Nazar, L.F.; *Chem. Mater*. **1996**, 8, 2005.

12. Bein, T.; Enzel, P.; *Angew. Chem. Int. Ed. Engl*. **1989**, *28*, 1692.

13. Lira-Cantú, M.; Gómez-Romero, P.; *Chem. Mater*. **1998**, *10*, 698.

14. Jang, S.H.; Han, M.G.; Im, S.S.; *Synth. Met*. **2000**, *110*, 17.

15. Mehrotra, V.; Keddie, J.L.; Miller, J.M.; Giannelis, E.P.; *J. Non-Crystalline Solids* **1991**, *136*, 97.

16. Wei, Y.; Yeh, J-M.; Jin, D.; Jia, X.; Wang, J.; Jang, G-W.; Chen, C.; Gumbs, R.W.; *Chem. Mater*. **1995**, 7, 969.

17. Hori, T.; Kuramoto, N.; Tagaya, H.; Karasu, M.; Kadokawa, J.; Chiba, K.; *J. Mater. Res*. **1999**, *14*7.

18. Ruiz-Hitzky, E.; Aranda, P.; *An. Quim-Int. Ed*. **1997**, *93*, 197.

19. Maia, D.J.; De-Paoli, M.A.; Alves, O.L.; Zarbin, A.J.G.; Neves, S.; *Quim. Nova* **2000**, *23*, 204.

20. Zarbin, A.J.G.; De-Paoli, M.A.; Alves, O.L.; *Synth. Met*. **1999**, *99*, 227.

21. Maia, D.J.; Zarbin, A.J.G.; Alves, O.L.; De-Paoli, M.A.; *Adv. Mater*. **1995**, *7*, 792.

22. Sotomayor, P.T.; Raimundo, I.M.; Zarbin, A.J.G.; Rohwedder, J.J.R.; Neto, G.O.; Alves, O.L.; *Sensor Actuact. B-Chem*. **2001**, *74*, 157.

23. Gonçalves, A.B.; Mangrich, A.S,; Zarbin, A.J.G.; *Synth. Met*. **2000**, *114*, 119.

24. Zarbin, A.J.G.; Maia, D.J.; De-Paoli, M.A.; Alves, O.L.; *Synth. Met*. **1999**, *102*, 1277.

25. Beleze, F.A.; Zarbin, A.J.G.; *J. Brazil. Chem. Soc*. **2001**, *12*, 542.

26. Maeda, S.; Armes, S.P.; *Chem. Mater*. **1995**, *7*, 171.

27. Tang, B.Z.; Geng, Y.H.; Lam, J.W.Y.; Li, B.S.; Jing, X.B.; Wang, X.H.; Wang, F.S.; Pakhomov, A.B.; Zhang, X.X.; *Chem. Mater*. **1999**, *11*, 1581.

28. Suri, K.; Annapoorni, S.; Sarkar, A.K.; Tandon, R.P.; *Sens. Actuact. B-Chem.* **2002**, *81*, 277.

29. Hao, Y.; Yang, M.; Yu, C.; Cai, S.; Liu, M.; Fan, L.; Li, Y.; *Solar Energy Mater. Solar Cells* **1998**, *56*, 75.

30. Feng, W.; Sun, E.; Fujii, A.; Wu, H.; Nihara, K.; Yoshino, K.; *Bull. Chem. Soc. Jpn*. **2000**, 73, 2627

31. Su, S-J.; Kuramoto, N.; *Synth. Met*. **2000**, *114*, 146.

32. Gurunathan, K.; Trivedi, D.C.; *Mater. Lett*. **2000**, *45*, 262.

33. Xia, H.; Wang, Q.; *Chem. Mater*. **2002**, *14*, 2158.

34. Nogueira, A.F.; Micaroni, L.; Gazotti, W.A.; De-Paoli, M.A.; *Electrochem. Commun*. **1999**, *1* 262.

35. Murakoshi, K.; Kogure, R.; Wada, Y.; Yanagida, S.; *Chem. Lett*. **1997**, 471.

36. Murakoshi, K.; Kogure, R.; Wada, Y.; Yanagida, S.; *Solar Energy Mater.Solar Cells* **1998**, *55*, 113.

37. Wang, G.; Chen, H.; Zhang, H.; Yuan, C.; Lu, Z.; Wang, G.; Yang, W.; *Appl. Surf. Sci*. **1998**, 135, 97.

38. Kobayashi, N.; Teshima, K.; Hirohashi, R.; *J. Mater. Chem*. **1998**, *8*, 497.

39. Avvaru, N.R.; Tacconi, N.R.; Rajeshwar, K.; *Analyst* **1998**, *123*, 113.

40. Schnitzler, D.C.; Meruvia, M.S.; Hummelgen, I.A.; Zarbin, A.J.G.; *Chem. Mater* **2003**, *15*, 4658.

41. Bischoff, B.L.; Anderson, M.A.; *Chem. Mater*. **1995**, *7*, 1772.

42. Oliveira, M.M.; Schnitzler, D.C.; Zarbin, A.J.G.; *Chem Mater* **2003**, *15*, 1903.

43. Pielichowski, K.; *Solid State Ionics* **1997**, *104*, 123.

44. Matveeva, E.S.; Calleja, R.D.; Parkhutik, V.P.; *Synth. Met*. **1995**, *72*, 105.

45. Han, M.G.; Lee, Y.J.; Byun, S.W.; Im, S.S.; *Synth. Met*. **2001**, *124*, 337.

46. Quillard, S.; Berrada, K.; Lovarn, G.; Lefrant, S.; Lapkowiski, M.; Pron, A.; *New J. Chem*. **1995**, *19*, 365.

47. Furukawa, Y.; Hara, T.; Hyoto, Y.; Harada, I.; *Synth. Met*. **1986,** *16,* 189.

48. Sariciftici, N.S.; Bartonek, M.; Kuzmany, H.; *Synth. Met*. **1989**, *29*, E193.

49. Louarn, G.; Lapkowski, M.; Quillard, S.; Pron, A.; Buisson, J.P.; Lefrant, S.; *J. Phys. Chem*. **1996**, *100*, 6998.

50. Engert, C.; Umapathy, S.; Kiefer, W.; Hamaguchi, H.; *Chem. Phys. Lett*. **1994**, *218*, 87.

51. Xia ,Y.; Wiesinger ,M.; MacDiarmid, A.G.; *Chem Mater*. **1995**, 7, 443.

52. Kuo, C-T.; Chen, C-H.; *Synth. Met*. **1999**, *99*,163.

53. Delime, F.; Léger, J.M.; Lamy, C.; *J. Appl. Electrochem*. **1998**, *28*, 27.

54. Zimer, A.M.; Bertholdo, R.; Grassi, M.T.; Zarbin, A.J.G.; Mascaro, L.H.; *Electrochem. Commun*. **2003**, *5*, 983